

# Neural Tissue Characterization using Integrated Relaxometry Analysis

A. Dula<sup>1</sup>, M. Does<sup>1</sup>

<sup>1</sup>Institute of Imaging Science, Vanderbilt University, Nashville, TN, United States

**Intro:** Integrated  $T_1$  and  $T_2$  characteristics of white matter in a rat brain were studied *in vivo* at 9.4T. Understanding micro anatomical structure of white matter is of distinctive value in determining the origin and establishment of image contrast in MRI. The characterization of multi-exponential  $T_1$  and  $T_2$  ( $MET_1, MET_2$ ) properties may permit quantification of the relative tissue fraction of the postulated components, myelin, in particular (1). Two water pool relaxation times and water pool fractions were calculated using a multi-echo, single-slice acquisition sequence at each of five inversion recovery times ( $T_1$ ). The shortest  $T_2$  component is commonly attributed to myelin, based on the relative component size and its correlation to the amount of water in the myelin. In addition, this component has been shown to disappear following a state of demyelination (2, 3). The remaining white matter components are intracellular and intercellular water. The observance of  $MET_1$  has been reported *in vivo* in peripheral nerve (4), but not yet in white matter of the brain.  $MET_1$  is more readily observed using integrated  $T_1$ - $T_2$  measurements as opposed to the conventional 1D inversion or saturation recovery sequences (5).

**Methods:** Male Sprague-Dawley rats with a typical weight of 150 g were anesthetized using isoflurane/oxygen gas mixture, induction at 5% and maintenance at 2%, while respiratory rate was measured. Body temperature was monitored using a rectal thermocouple and maintained near 37°C. Imaging was performed at 400 MHz on a Varian 9.4 T magnet with maximum gradient strength of 40 G/cm. A 38 mm litzcage coil was used for RF transmission and signal reception. Multi-echo, single-slice images were acquired ( $T_R/T_E = 3390/8$  ms) with five inversion times ( $T_1 = 0.01, 0.23, 0.55, 1.28, 3.00$ s) to perform integrated  $T_1$ - $T_2$  measurements. Thirty-two echoes were acquired with 8 averages to ensure a SNR > 220 for all inversion times. A data matrix of 96 x 96 was acquired over a 30 mm field of view (FOV), resulting in an approximate voxel size of 313  $\mu$ m x 313  $\mu$ m for the 2 mm slice. This imaging geometry was chosen to provide sufficient resolution in all three dimensions in an attempt to avoid partial-volume averaging of white matter and surrounding tissue. The resulting  $T_2$ -decay was analyzed using MATLAB, and fit to an exponential decay using a non-negative, least-squares method. The integrated areas of each  $T_2$  peak were fitted to Eq. [1], yielding a  $T_1$  estimate for each  $T_2$  component. Where the variable  $T_x = -T_R + T_E(N_E + 1/2)$ , which accounts for the multi-echo sequence contribution to  $T_1$  estimation.

$$M = abs(M_o * (1 + \exp(-T_x/T_1) - 2 * \exp(-T_x/T_1))) \quad [1] \quad A$$

The  $T_2$  spectra, seen in Figure 1A, were created by defining a broad and finely sampled  $T_2$  domain in conjunction with a minimum energy-smoothing constraint, performed iteratively with varied weighting of the constraint until the degree of smoothing is such that the spectrum contains no spurious components.

**Results:** The spectrum from white matter produced two peaks, with average  $T_1$ ,  $T_2$ , and fractional values shown Table 1. Analysis of gray matter resulted in a monoexponential decay and a single  $T_1$  value, while of white matter revealed two  $T_2$  components, consistent with previous studies (6), each of which had a unique  $T_1$  value. Typical IR curves for each white matter  $T_2$

component and gray matter are shown in Fig. 1B. The  $T_1$  value of the myelin  $T_2$  component is similar to that found from peripheral nerve (4). The multiexponential analysis of the MR signal will allow understanding of the  $T_1$  characteristics of myelin that could be useful in the design of and inversion recovery (IR) or double IR to observe myelin (6).

**Acknowledgements:** The authors would like to acknowledge financial support from the NIH, Grant # EB001744 as well as technical and animal assistance provided by Richard Beheza and Jarrod True.

- Vasilescu V., K.E., Simplaceanu V., Democo D. *Experientia*, 1977. **34**: p. 1443.
- Mackay, A., K. Whittall, J. Adler, D. Li, D. Paty, and D. Graeb. *Magnetic Resonance in Medicine*, 1994. **31**(6): p. 673.
- Does, M.D. and R.E. Snyder. *Magnetic Resonance in Medicine*, 1996. **35**(2): p. 207.
- Does, M.D. and J.C. Gore. *Magnetic Resonance in Medicine*, 2002. **47**(2): p. 274-283.
- Snaar, J.E.M. and H. Vanas. *Journal of Magnetic Resonance*, 1992. **99**(1): p. 139.
- Travis, A.R.D., M. D. *Proceedings of the International Society of Magnetic Resonance in Medicine Twelfth Scientific Meeting (Kyoto)*: p. 178.

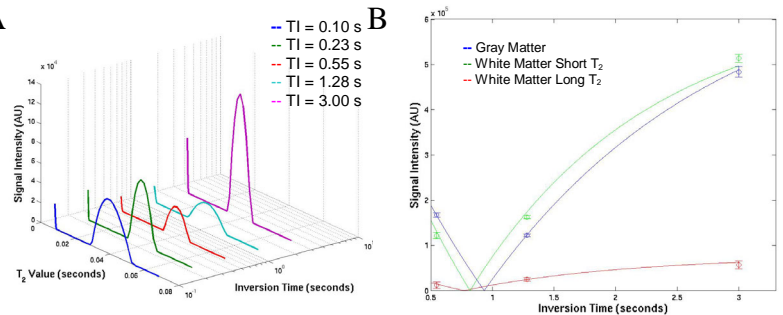


**Figure 1** - A) Spectrum for one integrated data set,  $T_1$  as indicated. B) Inversion recovery data with calculated fit values using Eq. [1], component indicated.

	$T_2$ (ms)	Fraction	$T_1$ (s)
<b>Short Component</b>	8.281 +/- 0.556	0.141 +/- 0.054	1.188 +/- 0.088
<b>Long Component</b>	37.685 +/- 3.520	0.859 +/- 0.088	1.453 +/- 0.140
<b>Gray Matter</b>	40.424 +/- 2.591	1.000 +/- 0.292	1.624 +/- 0.169

**Table 1** - Average  $T_1$ ,  $T_2$ , and fractional values with standard deviations. (n = 5)